

Electrochemical rewiring through quantum conductance effects in single metallic memristive nanowires – Supplementary Information

Gianluca Milano^{*1}, *Federico Raffone*^{*2}, *Katarzyna Bejtka*^{2,3}, *Ivan De Carlo*^{1,4}, *Matteo Fretto*¹,
Fabrizio Candido Pirri^{2,3}, *Giancarlo Cicero*², *Carlo Ricciardi*², *Ilia Valov*^{5,6}

¹Advanced Materials Metrology and Life Sciences Division, INRiM (Istituto Nazionale di Ricerca Metrologica), Strada delle Cacce 91, 10135 Torino, Italy.

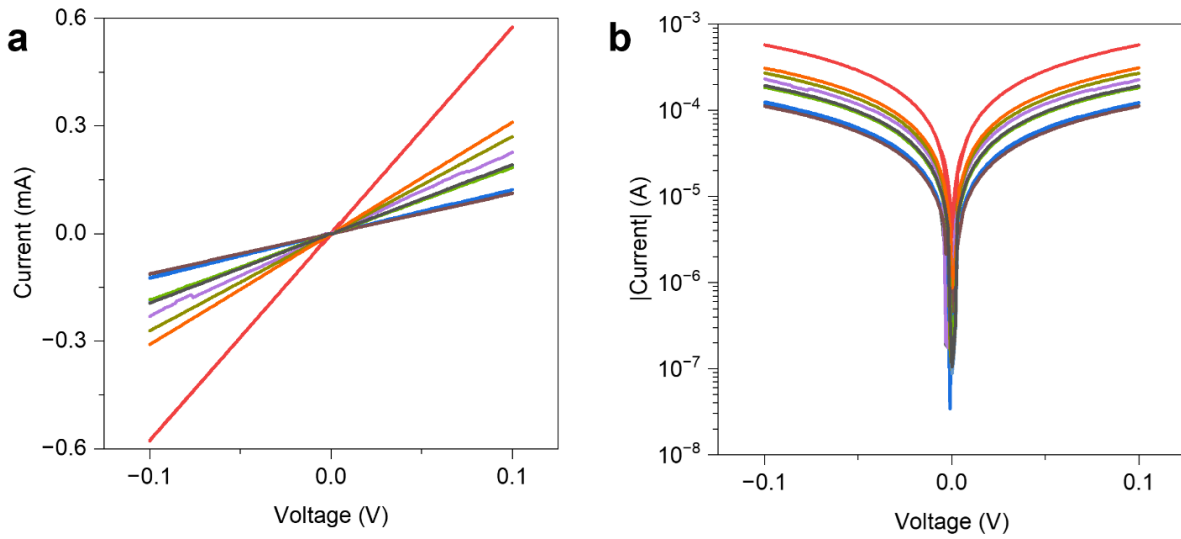
²Department of Applied Science and Technology, Politecnico di Torino, C.so Duca degli Abruzzi 24, 10129 Torino, Italy.

³Centre for Sustainable Future Technologies, Istituto Italiano di Tecnologia, Via Livorno 60, 10144 Torino, Italy.

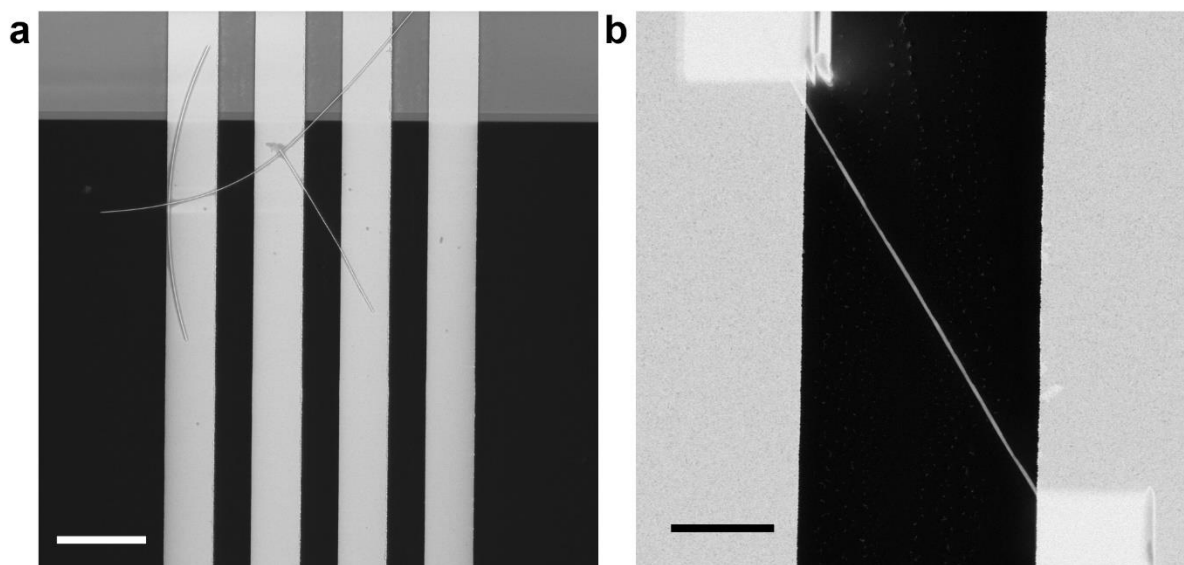
⁴Department of Electronics and Telecommunications, Politecnico di Torino, C.so Duca degli Abruzzi 24, 10129 Torino, Italy.

⁵Forschungszentrum Jülich, Institute of Electrochemistry and Energy System, WilhelmJohnen-Straße, 52428, Jülich, Germany.

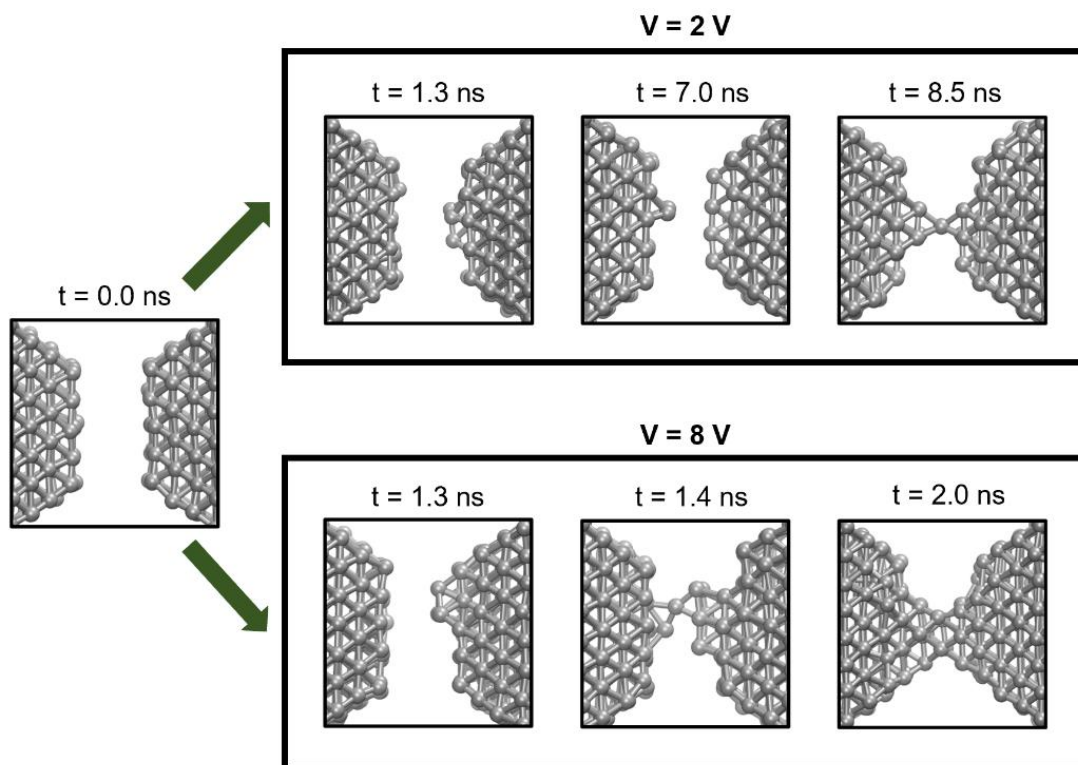
⁶“Acad. Evgeni Budevski” (IEE-BAS, Bulgarian Academy of Sciences (BAS), Acad. G. Bonchev Str., Block 10, 1113 Sofia, Bulgaria



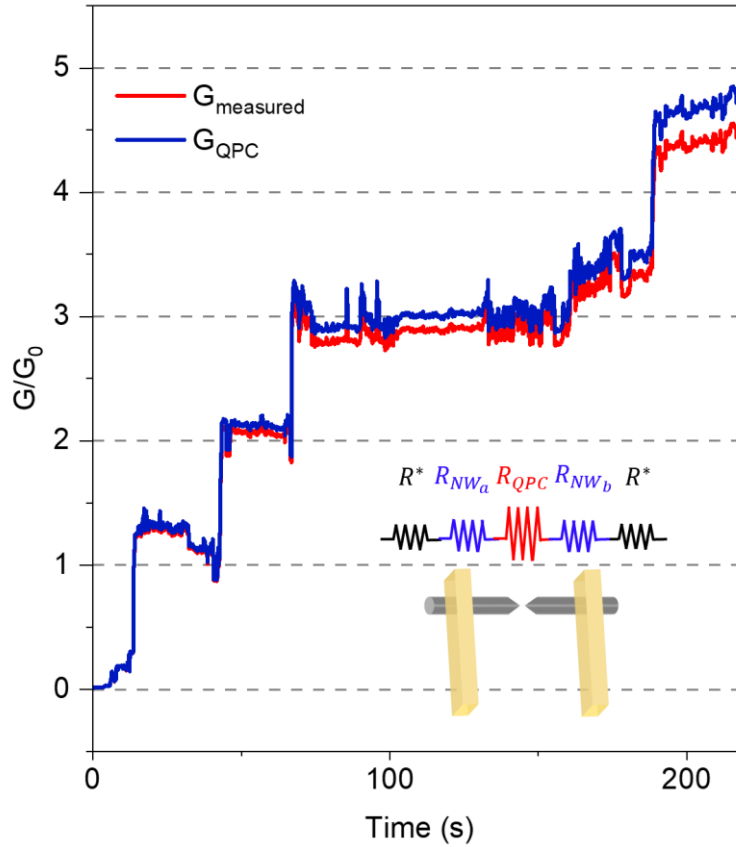
Supplementary Figure S1. Pristine state of single Ag NW memristive devices. (a) I - V characteristics and corresponding (b) I - V characteristics in log scale of 11 single Ag NW memristive cells in the pristine state. Pristine state resistance values range from 173 Ω to 895 Ω , as detailed in Supplementary Table 1.



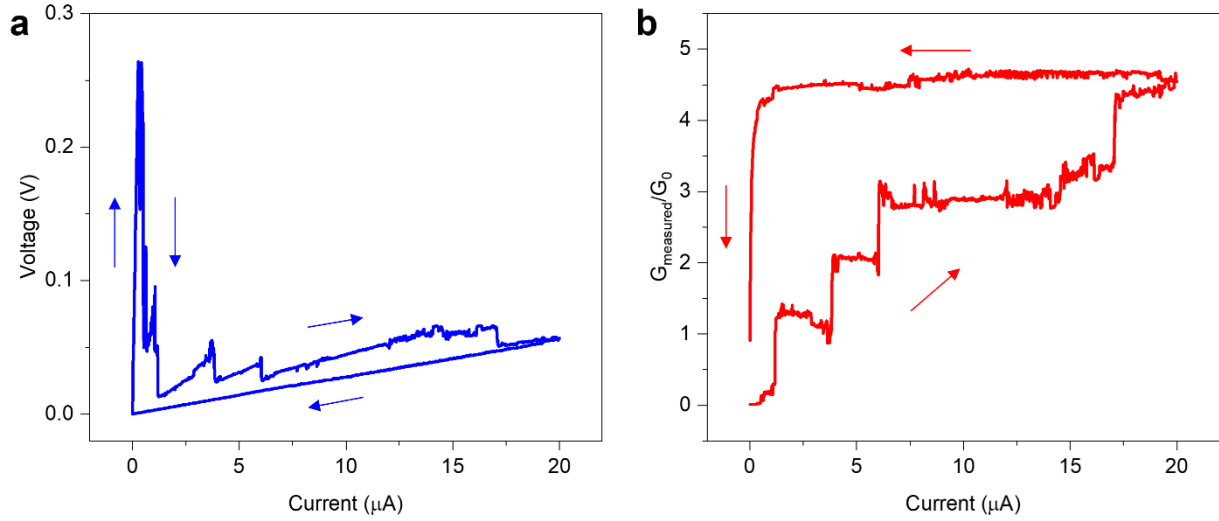
Supplementary Figure S2. *In-situ* TEM measurements. (a) FESEM image of the e-chip showing layout of the electrodes on the electron transparent SiN membrane with NW deposited on top (scale bar, 10 μm). (b) STEM image of an Ag NW device before in situ electrical characterization, realized by contacting the NW with underlying electrodes with a Pt deposition (scale bar, 20 μm). The NW device was realized by contacting the NW deposited in between central electrodes reported in panel a.



Supplementary Figure S3. Effect of the applied voltage on filament formation. Despite the filament formation occurs by following the same formation stages, an increase of the applied voltage results in faster dynamics since the applied voltage increase the kinetics. As an example, the establishment of the first single atom bridge between the two tips occurs faster by applying 8V respect to the case when 2V are applied.



Supplementary Figure S4. Effect of parasitic resistances on quantum conductance levels. (a) Example of the comparison of the measured conductance ($G_{measured}$) and the QPC conductance obtained by subtracting the effect of parasitic resistances (G_{QPC}), where the resistance R_{QPC} was evaluated through the relationship $R_{QPC} \approx R_{measured} - R_{pristine}$ (details in Supplementary Note 1). The pristine state resistance of the considered NW was $\sim 173 \Omega$ (NW#2 in Supplementary Table 1) while the conductance time trace refers to the one reported in Figure 3a. In this context, it is worth noticing that device-to-device variations in the influence of parasitic resistances on quantum conductance levels rely on different measured parasitic resistance values (i.e., different measured NW pristine state resistance).



Supplementary Figure S5. Hysteretic memory effect. (a) V - I characteristic of a single NW during the SET process showing a hysteretic memory behavior when stimulated with a current sweep $0 \rightarrow 20 \rightarrow 0 \mu\text{A}$ and (b) Corresponding hysteretic behavior of the device conductance. Differently from what expected from conventional QPC phenomena related to purely electronic mechanisms where V - I traces are expected to overlap during $0 \rightarrow 20 \mu\text{A}$ and $20 \rightarrow 0 \mu\text{A}$ current sweeps, the observed hysteretic memory behavior demonstrate that quantum levels rely on the reconfiguration of the atomic structure of the conductive filaments across the nanogap.¹

Supplementary Table 1. Pristine state resistance values. Pristine state resistance values of 11 single Ag NW memristive cells extracted from *I-V* characteristics reported in Supplementary Figure S1.

Device	Pristine state resistance (Ω)
NW #1	881
NW #2	173
NW #3	810
NW #4	434
NW #5	527
NW #6	895
NW #7	369
NW #8	322
NW #9	535
NW #10	540
NW #11	517

Supplementary Note 1. Subtraction of parasitic resistance effects on the nanogap resistance.

By considering the electrical circuital representations of the NW device before and after breakdown reported in Figure 1b, under the approximation that the resistance at the Pt -Ag NW interface R^* and that the overall resistance of the NW is not altered before and after breakdown ($R_{NW_a} + R_{NW_b} \approx R_{NW}$), the gap resistance R_{gap} can be evaluated as $R_{gap} \approx R_{measured} - R_{pristine}$. Since electrochemical rewiring/rupture of conductive filaments across the nanogap causes the lowering/increasing of R_{gap} , the resistance of quantum levels associated to the formation/rupture of these conductive filaments can be evaluated in first approximation through the relationship $R_{gap} \approx R_{QPC} \approx R_{measured} - R_{pristine}$. This allows the estimation of the conductance quantum plateaus by subtracting the effect of parasitic resistances.

REFERENCES

- (1) Milano, G.; Aono, M.; Boarino, L.; Celano, U.; Hasegawa, T.; Kozicki, M.; Majumdar, S.; Menghini, M.; Miranda, E.; Ricciardi, C.; Tappertzhofen, S.; Terabe, K.; Valov, I. Quantum Conductance in Memristive Devices: Fundamentals, Developments, and Applications. *Advanced Materials* **2022**, *34* (32), 2201248. <https://doi.org/10.1002/adma.202201248>.